



ELSEVIER

Contents lists available at ScienceDirect

Micro and Nano Engineering

journal homepage: www.journals.elsevier.com/micro-and-nano-engineering

Research paper

Hierarchically structured polydimethylsiloxane films for ultra-soft neural interfaces

Bekim Osmani^{a,*}, Helmut Schiff^b, Konrad Vogelsang^b, Raphael Guzman^c,
Per Magnus Kristiansen^d, Rowena Crockett^e, Aarati Chacko^e, Simon Bucher^a, Tino Töpfer^a,
Bert Müller^a

^a Biomaterials Sciences Center, Department of Biomedical Engineering, University of Basel, Allschwil, Switzerland^b Laboratory for Micro- and Nanotechnology, Paul Scherrer Institute, Villigen PSI, Switzerland^c Department of Neurosurgery, University Hospital Basel, Basel, Switzerland^d Institute of Polymer Nanotechnology, FHNW University of Applied Sciences and Arts Northwestern Switzerland, Windisch, Switzerland^e Empa, Swiss Federal Laboratories for Materials Science and Technology, Dübendorf, Switzerland

ARTICLE INFO

Keywords:

Compliant neural interfaces
Conductive elastomers
PEEK films
Thermal nanoimprint lithography
Brain and spinal cord modulation
Nanometer-thin silicone gold composite

ABSTRACT

Long-term interfacing with neural tissue is key for the diagnosis and therapy of neurological disorder. Coatings with dedicated micro- and nanostructures have been proposed, such as gold nanowires, platinum nanostructured by electrochemical roughening, columnar and porous titanium nitride, carbon nanotubes, and conductive polymers. The performance of these coatings, however, is limited because of the mechanical mismatch between implant and neural tissue. Herein, we show that micro- and nanostructured, soft and conductive elastomer films can be obtained by depositing gold on nanometer-thin thiol-functionalized polydimethylsiloxane (PDMS) films. Additionally, microstructured polyether ether ketone (PEEK) films enable directional ordering in topology. The formation of soft and conductive PDMS films with oriented wrinkles on the macroscopic scale was controlled by the ratio between the metal/elastomer thicknesses and the depth of thermally imprinted trenches. Four-point probe measurements revealed that the electrical conductivity is one order of magnitude higher than that of recently presented hydrogel formulations. Nano-indentations proved that the submicrometer-thin conductive elastomer exhibit an average elastic modulus well below 10 MPa. This material system can be made tens of micrometers thin, and, therefore, has the potential to address several challenges of current implantable neural interfaces for the central nervous system, e.g. fabrication of softer and more flexible micrometer-thin spinal cord arrays.

1. Introduction

Recently, there has been growing excitement around treating neurological diseases and spinal cord injuries using neuromodulation techniques [1,2]. Several studies reported on non-invasive transcranial direct current stimulation (tDCS) regarding Parkinson's disease, other movement disorders, motor stroke, poststroke aphasia, multiple sclerosis, epilepsy, Alzheimer's disease, tinnitus, depression, schizophrenia, and craving/addiction [3]. Invasive neuro-modulation methods can target more specific and deeper regions of the brain compared to non-invasive transcranial current stimulations [4]. The treatment success, however, is limited by the lack of appropriate tools to probe the nervous system [5,6]. The elastic modulus of state-of-the-art platinum-iridium or titanium electrodes, which represent the actual

neural interface, differs by orders of magnitude from that of neural tissue [7]. The hard implant is constantly exposed to pulsatile micrometer-motions injuring to the surrounding neural tissue and, therefore, inducing a foreign body response and the formation of glial scar tissue [6]. Electrical stimulation may still work at elevated voltages, however with a sacrifice in recording capability and with a loss in spatial resolution [8]. Recently developed conductive and soft neural interfaces were reducing the gap of the mechanical mismatch between the man-made system and the neural tissue [7,9,10]. Tybrandt et al. proposed a soft composite of gold-coated titanium dioxide nanowires embedded in a silicone matrix [11]. Choi et al. presented nano-composite compounds of ultralong gold-coated nanowires in an elastomeric block copolymer matrix [12]. Conductive and ultrasoft poly (3,4-ethylenedioxythiophene) polystyrene sulfonate (PEDOT:PSS) hydrogels are

* Corresponding author.

E-mail address: bekim.osmani@unibas.ch (B. Osmani).<https://doi.org/10.1016/j.mne.2020.100051>

Received 14 February 2020; Received in revised form 26 March 2020; Accepted 31 March 2020

2590-0072/ © 2020 The Authors. Published by Elsevier B.V. This is an open access article under the CC BY license (<http://creativecommons.org/licenses/by/4.0/>).

promising as they mimic the mechanical properties of neural tissue [13–15]. The common weaknesses of such hydrogel systems, however, are the delamination from the carrier/substrate and their restricted electrical conductivity [16]. Chen and coworkers stated that a soft and flexible electrode communicating with the nervous system over a long-term scale remains to be demonstrated [5]. Further challenges of future biomimetic and soft electrodes include functionalization by e.g. chemical modification, a strong adhesion of the electrode to the substrate, and the achievement of appropriate signal-to-noise ratio for a reasonable time period *in vivo*.

PDMS films can be made soft, biocompatible and processed via manifold fabrication routes, such as spin coating, electro-spraying, molecular beam deposition, and 3D-printing [17–19]. Silicone fluids can be modified, for example by functionalization with thiol groups, which allow for covalent bonding to gold. The elastic modulus of the modified silicones can be tuned employing ultraviolet light radiation [20]. Nanometer-thin thiol-functionalized silicone films become conductive after the deposition of 50 nm gold as these atoms diffuse into the elastomeric network and covalently bind to the thiol groups [21]. The topology of PDMS films can be controlled via oxygen plasma treatment and depends on the film thickness and the process parameters [22,23]. It has been shown that the resulting wrinkles align along edges due to stress relaxation phenomena [24]. The edges can be easily introduced via micron-sized gratings using thermal nanoimprint lithography (NIL), which is one of the most cost-effective methods for replicating microstructures into thermoplastics [25].

Herein, we present a soft, ultra-thin, conductive, functionalized PDMS film on a NIL-patterned thermoplastic polymer. The deposited gold is strongly bonded by chemisorption or even covalent bonds to the thiol groups within the 350 nm-thin PDMS film. First, a titanium film fabricated by high-power impulse magnetron sputtering (HiPIMS) serves as an adhesive interface between the PDMS film and the underlying microstructured thermoplastic film. The microstructures increase the contact area and therefore improve the adhesion of the titanium film to the thermoplastic polymer. Second, the micro-trenches enable a mechanical interlocking of the PDMS film and hence improve the stability of the material system. Third, NIL-patterned microstructures increase the effective surface and define the final topology of the conductive PDMS film. The subsequent oxygen plasma treatment produces nanometer-sized corrugations aligned perpendicular to the trenches. The NIL surface patterning thus allows for control over the orientation of the corrugations. Human tissues also exhibit such anisotropic structural features. Therefore, the material system presented not only provides comparatively high surface areas, but also a sound basis for a prospective biomimetic platform for long-term interfacing with human neural tissue.

This thin-film technology may enable very thin spinal cord arrays which can withstand harsh pressures of the spine. Spinal cord stimulation (SCS) is known to help manage chronic back, leg, or arm pain even when other therapies have failed. Currently, thin wires, termed leads, or 2 mm-thick paddles connected to a pulse generator are implanted in the back. Their performance, however, is suboptimal because of the limited spatial resolution, lead migration, and local compression of the spinal cord.

2. Material and methods

2.1. Microstructuring polymer films via NIL

Commercially available PEEK films with thicknesses of 125, 250 and 500 μm , $T_g = 187\text{ }^\circ\text{C}$ (Aptiv™ 1000 series, Victrex Europa GmbH, Hofheim, Germany), poly(methyl methacrylate) (PMMA) 175 μm thick, $T_g = 113\text{ }^\circ\text{C}$ (Plexiglas® film 99,524, Evonik Performance Materials GmbH, Darmstadt, Germany) and polyethylene naphthalate (PEN) films 125 μm -thick, $T_g = 121\text{ }^\circ\text{C}$ (Teonex® Q51, Synflex Elektro GmbH, Blomberg, Germany) were used. These films were surface patterned

with micron-sized gratings using thermal NIL in a precision hot press (HEX03, Jenoptik AG, Jena, Germany) at temperatures between 180 and 280 $^\circ\text{C}$ with a pressure of 20 kN for a period of ten minutes and subsequently cooled down with an average rate of 0.25 K/s. Afterwards, they were taken out of the press and demolded at room temperature. Silicon substrates with 800 nm deep surface topographies, 2 and 5 μm lines and squares with vertical side-walls, were used as stamps.

2.2. Adhesive conductive track

Prior to metallization, the polymer films were oxygen plasma-treated for ten minutes at a power of 100 W with a frequency of 40 kHz and 10 sccm oxygen flow rate (FEMTO System, Diener Electronics, Ebhausen, Germany). The HiPIMS metallization process was carried out using a chopped pulse comprising of eight 25 μs pulses interspersed by 100 μs rest periods and a total pulse period of 5000 μs , which corresponds to 200 Hz pulse frequency and 4% duty cycle [26]. The pulsing was achieved using a Melec SIPP2000USB-Dual pulser (Melec GmbH, Baden-Baden, Germany) and an ADL GX 50/1000 DC power supply (ADL Analoge & Digitale Leistungselektronik GmbH, Darmstadt, Germany) attached to a Grade 2 titanium target [27]. The process voltage was set to 588 V, which corresponded to 2.1 A and 1.3 kW. The base pressure prior to deposition was 1.1×10^{-6} mbar at room temperature (22 $^\circ\text{C}$). The deposition was carried out in 6 μbar argon (6.0 purity) environment, which corresponds to ~ 82 sccm flow rate in this chamber, with the gas introduced at the magnetron. The substrate was not actively heated, but deposition-related heating resulted in a maximum temperature of 96.5 $^\circ\text{C}$.

2.3. Fabrication of nanometer-thin conducting PDMS films

For the (350 \pm 50) nm-thin PDMS film, a dimethyl silicone elastomer containing mercaptopropyl (-SH) side groups with an average molecular weight of 1900 g/mol (KF-2001, Shin-Etsu Silicones Europe, The Netherlands) was spin-coated (WS 400B-6NPP/LITE/AS, Laurell Technologies Corporation, North Wales, PA, USA) at a rotation speed of 8000 rpm for eight minutes. The PDMS films were crosslinked using a 200 W Hg-Xe-UV lamp (Super-quiet mercury-xenon lamp L2423, Hamamatsu Photonics K.K., Hamamatsu, Japan) mounted at a distance of 20 cm from the specimen. Subsequently, a nominal thickness of 50 nm gold (Q300T D Plus, Quorum Technologies, UK) was deposited at a discharge current of 150 mA for a period of 30 s. The specimens were oxygen plasma-treated at 200 W for a period of 30 s at a frequency of 40 kHz (PICO System, Diener Electronics, Ebhausen, Germany). The oxygen partial pressure was kept at 0.3 mbar at a flow rate of 25 sccm.

2.4. AFM imaging and nanoindentations

The topology was extracted by raster-scanning the surface with a soft AFM probe (Tap190Al-G probe, NanoAndMore GmbH, Wetzlar, Germany) in tapping mode (vibration amplitude of 420 nm, set point 70%) using a FlexAFM System (Nanosurf AG, Liestal, Switzerland). For each image, 512 lines were acquired at a speed of one line per second. The raw data were levelled by subtracting a mean plane and removing a polynomial background of third degree using the open source software for SPM data analysis Gwyddion, Version 2.41. The elastic moduli were derived from AFM-based nanoindentation experiments using a cantilever with a spherical tip having a e-beam processed radius of (149 \pm 4) nm (B150_CONTR, Nanotools GmbH, Germany). The spring constant $k = (0.38 \pm 0.05)$ N/m of the AFM cantilever was determined using the Sader method [28]. The dimensionless Tabor parameter $\mu = (R\gamma^2/E^2\varepsilon^3)^{1/3}$ has been calculated to select the appropriate contact model [29]. Here, R is the probe radius, γ the adhesion work and ε the equilibrium separation, typically in the range of 0.5 nm. Using $R = 149$ nm and the average pull-off force $F_0 = 35$ nN, the adhesion work $\gamma = F_0/(3\pi R/2)$ is found to be 49 mJ/m². For $\mu > 5$,

the Johnson-Kendall-Roberts (JKR) contact model, taking into account adhesion forces between the spherical tip and the electrode, is recommended [29,30]. The JKR model is implemented in Artidis® software (Artidis, Basel, Switzerland), offering a fully automated post-processing and analysis of the data. Spots of $60 \times 60 \mu\text{m}^2$ were partitioned into 14'400 domains, each serving as nano-indentation site.

2.5. Four-point measurements

The sheet resistance was quantified using the four-point setup. The advantage of four-terminal sensing is that the resistances of wires, contacts and the internal resistance of the two-terminal sensing are eliminated. Four liquid metal drops (Coollaboratory Liquid Pro, Coollaboratory, Magdeburg, Germany) were placed at equal distances. The probe tips were mounted on micropositioners (Signatone, APS Solutions GmbH, Munich, Germany) and were lowered contacting the liquid metal drops. A constant current of 0.1 to 1.0 mA was applied to the outer tips using a commercially available source meter (Keithley 2401). The voltage drop between the inner tips was measured using a multimeter (Agilent 34461A Truevolt).

3. Results and discussion

When fabricated on thermally imprinted microstructures, the nanometer-thin conducting elastomer films exhibited oriented nanostructures. Fig. 1 schematically displays the necessary fabrication steps. It also shows the obtained surface structures of the nano-engineered neural interfaces (NENI) prototype. The conducting elastomer film consists of a 350 nm-thin thiol-functionalized PDMS film with embedded gold. These gold clusters correspond to a nominally 50 nm thin film. As shown previously, the gold has been incorporated into the elastomer network via covalent bonding to thiol sites [21]. In addition, the PDMS film improved the adhesion to the HiPIMS sputtered titanium film and therefore enable an irreversible bonding to the microstructured polymer substrate [31–33].

As a result of wetting, liquid PDMS film filled up the microstructures for features below $1 \mu\text{m}$ in size, see profiles in Fig. 1. The nano-wrinkles on the film's surface arise from the plasma-treatment. They can be tailored selecting the plasma intensity and the duration of the treatment [23]. The structures were oriented for trench widths up to $10 \mu\text{m}$.

Fig. 2 presents the topology of conductive elastomer films on microstructures with selected periodicity and depth. If the trench depth corresponded to the thickness of the PDMS layer deposited, we found parallel wrinkles, cf. images in Fig. 2 (B) and (C). Because the periodicity and amplitude of the nano-wrinkles depend on the elastomer thickness, the regions with higher amplitude and increased periodicity correspond to the darker trenches in the images of Fig. 2 (B) and (C) [23].

Fig. 2 (D) displays an AFM image and the corresponding FOURIER transform of the NENI prototype, shown in Fig. 1. The periodicity of the wrinkles $\lambda_{\text{wrinkles}} = (830 \pm 40) \text{ nm}$ relates to the profile D-D' (here measured between the ridges). The periodicities with $\lambda_1 = 16 \mu\text{m}$, $\lambda_2 = 8 \mu\text{m}$, and $\lambda_3 = 4 \mu\text{m}$, and $\lambda_3 = 2 \mu\text{m}$ correspond to the underlying microstructures along the profile E-E'. Due to stress-relaxation at the step edges of the substrate's microstructure, the observed nanowrinkles are aligned perpendicular to the edges. The ordering was more pronounced on the top of the $2 \mu\text{m}$ -broad ridges, and less between ridges. This behavior could help to preferentially orient the adherent neurons.

Fig. 3 represents stiffness maps of the NENI prototype derived from nanoindentation experiments. The elastic modulus locally varied between 6 and 12 MPa. This spatial dependence related to the substrate microstructure and gave rise to the bi-modal elastic modulus distribution with maxima at $E_1 = (8.1 \pm 1.8) \text{ MPa}$ and $E_2 = (9.4 \pm 1.6) \text{ MPa}$. The plasma induced nano-wrinkles of the PDMS film led to stiffer protrusions and softer impressions [34].

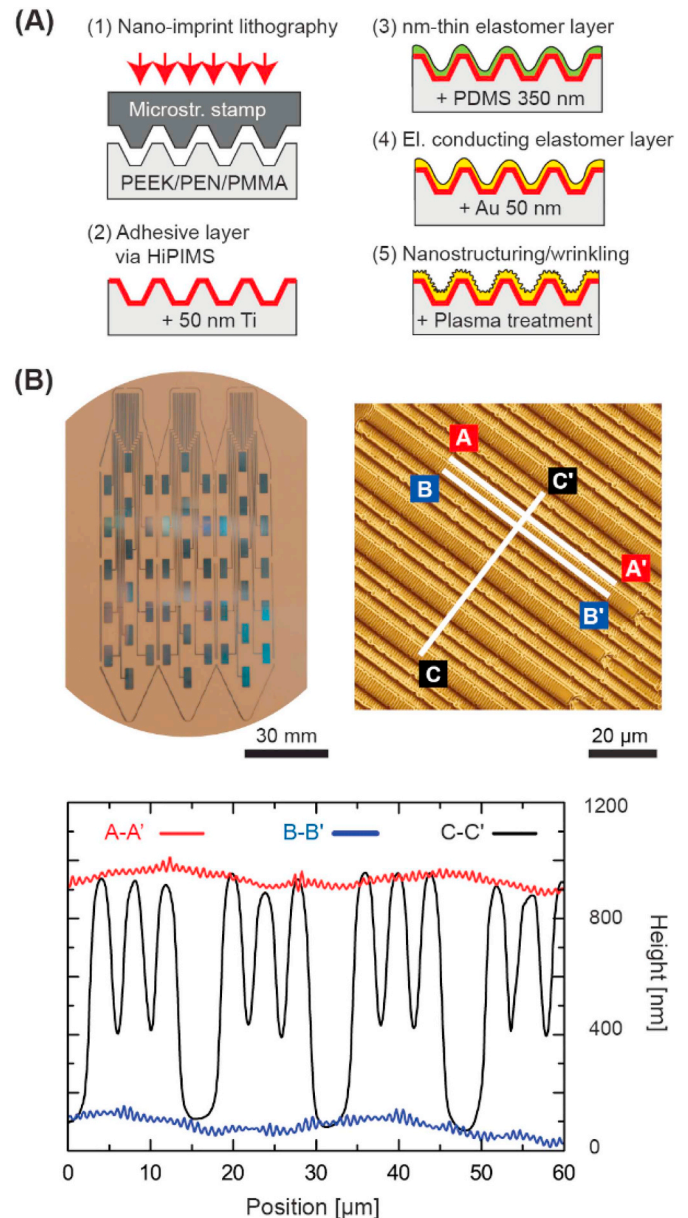


Fig. 1. Nano-Engineered Neural Interfaces - NENI. (A) Scheme of the five fabrication steps. (B) Top left: Photograph of a proof-of-concept prototype using PEEK films. The thin-film technology enables ultra-thin spinal cord arrays that can withstand the pressure of the spine. Electrical contacts to an implantable pulse generator (IPG) will be established via micromachining techniques. The insulated gold wires with a nominal diameter of about $50 \mu\text{m}$ will be welded to the NENI paddle. Top right: $90 \times 90 \mu\text{m}^2$ AFM scan of the electrode surface and corresponding cross-sections perpendicular and parallel to the microstructured ridges (bottom). The thermally imprinted microstructures were covered by aligned nano-wrinkles. (For interpretation of the references to colour in this figure legend, the reader is referred to the web version of this article.)

Four-point measurements of the NENI electrodes revealed a sheet resistance $R_s = (47.5 \pm 1.1) \Omega/\text{sq}$. With an electrode thickness of $(350 \pm 50) \text{ nm}$ the conductivity σ was found to be $(607 \pm 76) \text{ S/cm}$, cf. Fig. 4. This value is one order of magnitude larger than that for PEDOT:PSS hydrogels (40 S/cm) [14]. The underlying titanium oxide layer was essentially non-conductive.

4. Conclusions

The embedding of gold into thiol-functionalized silicone enables the

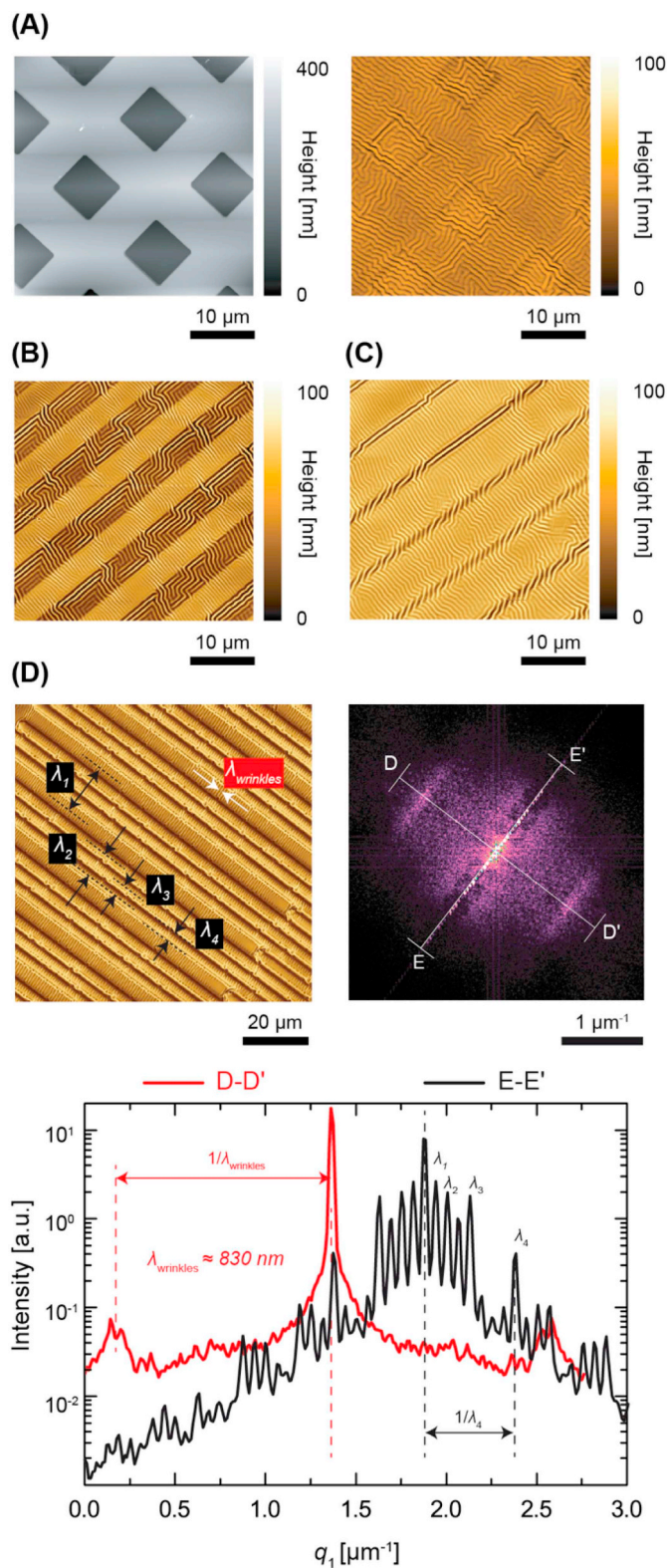


Fig. 2. Topology of micro- and nanostructured conductive elastomer films visualized by atomic force microscopy. (A) Surface of a thermally imprinted PEN substrate (left) and coated with a conductive elastomer film (right). (B, C) Nano-wrinkles of conductive PDMS with tailored degree of orientation based on the underlying microstructures (D) Formation of a nano-wrinkled conductive elastomer film on imprinted thermoplastic film (left) and corresponding Fourier transform (right). The observed intensity distribution relates to the periodicities of the thermally-imprinted substrate orientated perpendicular to each other. (Bottom) Profiles extracted from the Fourier transform.

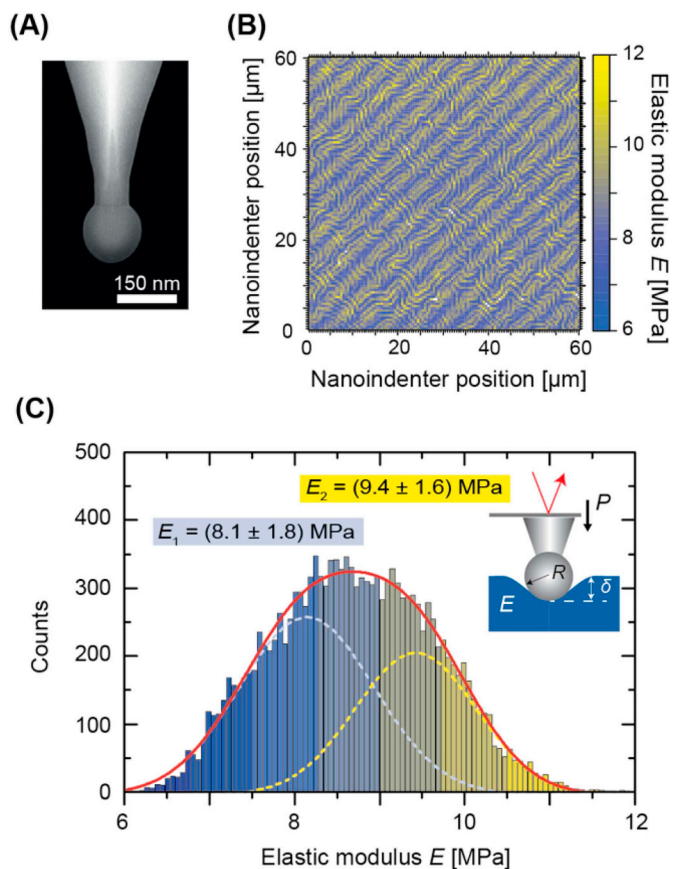


Fig. 3. Mechanical properties of the NENI electrodes. (A) Scanning electron microscopy image of the utilized spherical nanoindentation-probe with a radius of (149 ± 4) nm. (B) Nanomechanical map extracted from 14'400 nanoindentations on a $60 \times 60 \mu\text{m}^2$ area using the JKR contact model exhibiting topology-related elastic modulus modulations. (C) The related histogram reveals a bimodal stiffness distribution with maxima at $E_1 = (8.1 \pm 1.8)$ MPa and $E_2 = (9.4 \pm 1.6)$ MPa. Insert: Scheme of AFM-based nanoindentation using a spherical tip with a force $P = 50$ nN.

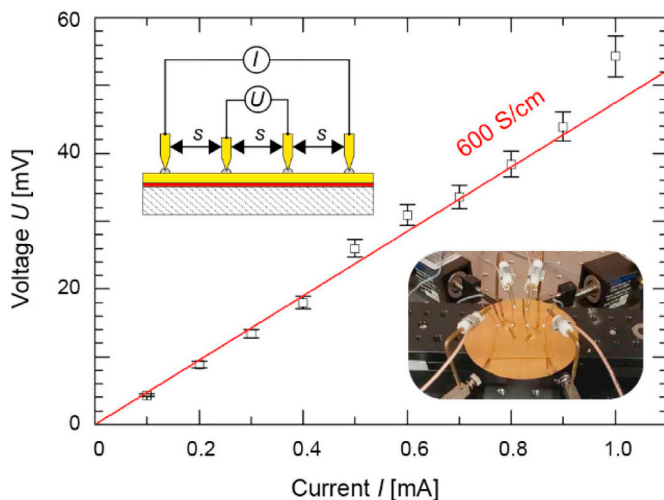


Fig. 4. Conductivity of the NENI electrode: The slope of the I - U curve, i.e. the sheet resistance R_s , resulted in a conductivity of (607 ± 76) S/cm considering an electrode thickness of 350 nm. Insert top: Scheme of the four-point conductivity measurement with liquid metal droplets contacting the soft NENI electrode. Insert bottom: Photograph of the experimental setup.

formation of long-term stable nanometer-thin films with a conductivity of ~ 600 S/cm and an elastic modulus below 10 MPa. Using the hierarchical structuring, i.e. thermal nano-imprint lithography for placing microstructures and oxygen plasma treatment for inducing nano-wrinkles, one obtains anisotropic properties known from human tissues. Consequently, this material system should form a soft interface. However, to obtain a flexible implant which conforms to small radii-3D-topologies in the brain or bend around the spinal cord, the PEEK films have to be micrometer-thin and eventually contain micro-perforations.

Declaration of Competing Interest

None.

Acknowledgements

The financial support of the Gebert R uf Foundation, Switzerland, Grant-ID GRS-058/18 and the Technology Transfer Office of the Universities of Basel, Bern and Z urich - Unictetra, Switzerland, Grant-ID UA-19/046 PoC Funding are gratefully acknowledged. The authors wish to thank Victrex (UK) for kindly providing PEEK films and Shin-Etsu Silicones Europe (NL) for kindly providing mercapto modified silicone fluids at no charge. The authors also wish to thank Sascha Martin from the mechanical workshop at the Department of Physics, University of Basel, for fabricating shadow masks for the deposition of electrodes.

Appendix A. Supplementary data

Supplementary data to this article can be found online at <https://doi.org/10.1016/j.mne.2020.100051>.

References

- [1] H.F. Iaccarino, et al., Gamma frequency entrainment attenuates amyloid load and modifies microglia, *Nature* 540 (2016) 230.
- [2] F.B. Wagner, et al., Targeted neurotechnology restores walking in humans with spinal cord injury, *Nature* 563 (2018) 65–71.
- [3] J.P. Lefaucheur, et al., Evidence-based guidelines on the therapeutic use of transcranial direct current stimulation (tDCS), *Clin. Neurophysiol.* 128 (2017) 56–92.
- [4] D.W. Scharre, et al., Deep brain stimulation of frontal lobe networks to treat Alzheimer's disease, *J. Alzheimers Dis.* 62 (2018) 621–633.
- [5] R. Chen, A. Canales, P. Anikeeva, Neural recording and modulation technologies, *Nat. Rev. Mater.* 2 (2017) 16093.
- [6] S.P. Lacour, G. Courtine, J. Guck, Materials and technologies for soft implantable neuroprostheses, *Nat. Rev. Mater.* 1 (2016) 16063.
- [7] N. Chen, et al., Neural interfaces engineered via micro- and nanostructured coatings, *Nano Today* 14 (2017) 59–83.
- [8] D.R. Merrill, M. Bikson, J.G. Jefferys, Electrical stimulation of excitable tissue: design of efficacious and safe protocols, *J. Neurosci. Methods* 141 (2005) 171–198.
- [9] J. Rivnay, H. Wang, L. Fenno, K. Deisseroth, G.G. Malliaras, Next-generation probes, particles, and proteins for neural interfacing, *Sci. Adv.* 3 (2017) e1601649.
- [10] J.W. Jeong, et al., Soft materials in neuroengineering for hard problems in neuroscience, *Neuron* 86 (2015) 175–186.
- [11] K. Tybrandt, et al., High-density stretchable electrode grids for chronic neural recording, *Adv. Mater.* 30 (2018) 1706520.
- [12] S. Choi, et al., Highly conductive, stretchable and biocompatible Ag–Au core–sheath nanowire composite for wearable and implantable bioelectronics, *Nat. Nanotechnol.* 13 (2018) 1048–1056.
- [13] Y. Liu, et al., Soft and elastic hydrogel-based microelectronics for localized low-voltage neuromodulation, *Nat. Biomed. Eng.* 3 (2019) 58.
- [14] B. Lu, et al., Pure PEDOT: PSS hydrogels, *Nat. Commun.* 10 (2019) 1043.
- [15] A.K. Gaharwar, N.A. Peppas, A. Khademhosseini, Nanocomposite hydrogels for biomedical applications, *Biotechnol. Bioeng.* 111 (2014) 441–453.
- [16] C. Kleber, M. Bruns, K. Lienkamp, J. R uhe, M. Asplund, An interpenetrating, microstructurable and covalently attached conducting polymer hydrogel for neural interfaces, *Acta Biomater.* 58 (2017) 365–375.
- [17] F.M. Weiss, et al., Electrospinning nanometer-thin elastomer films for low-voltage dielectric actuators, *Adv. Electron. Mater.* 2 (2016) 1500476.
- [18] T. T opper, et al., Time-resolved plasmonics on self-assembled hetero-nanostructures for soft nanophotonic and electronic devices, *Adv. Electron. Mater.* 3 (2017) 1700073.
- [19] A. Poulin, S. Rosset, H. Shea, Fully printed 3 microns thick dielectric elastomer actuator, *Proc. SPIE* 9798 (2016) 97980L.
- [20] B. Osmani, T. T opper, M. Siketanc, G. Kovacs, B. M uller, Electrospinning and ultraviolet light curing of nanometer-thin polydimethylsiloxane membranes for low-voltage dielectric elastomer transducers, *Proc. SPIE* 10163 (2017) 101631E.
- [21] B. Osmani, T. T opper, B. M uller, Conducting and stretchable nanometer-thin gold/thiol-functionalized polydimethylsiloxane films, *J. Nanophoton.* 12 (2018) 033006.
- [22] A. Schweikart, A. Fery, Controlled wrinkling as a novel method for the fabrication of patterned surfaces, *Microchim. Acta* 165 (2009) 249–263.
- [23] B. Osmani, G. Gerganova, B. M uller, Biomimetic nanostructures for the silicone-biosystem interface: Tuning oxygen-plasma treatments of polydimethylsiloxane, *Eur. J. Nanomed.* 9 (2017) 69–77.
- [24] N. Bowden, W.T.S. Huck, K.E. Paul, G.M. Whitesides, The controlled formation of ordered, sinusoidal structures by plasma oxidation of an elastomeric polymer, *Appl. Phys. Lett.* 75 (1999) 2557–2559.
- [25] H. Schiff, Nanoimprint lithography: 2D or not 2D? A review, *Appl. Phys. A Mater. Sci. Process.* 121 (2015) 415–435.
- [26] P.M. Barker, E. Lewin, J. Patscheider, Modified high power impulse magnetron sputtering process for increased deposition rate of titanium, *J. Vac. Sci. Technol.* 31 (2013) 060604.
- [27] E. Kessler, On the measurement of the heat of condensation of Ag, Bi, Sb, and Pb, *Phys. Status Solidi* 116 (1989) K61–K64.
- [28] E.S. John, W.M.C. James, M. Paul, Calibration of rectangular atomic force microscope cantilevers, *Rev. Sci. Instrum.* 70 (1999) 3967–3969.
- [29] Y.M. Efremov, D.V. Bagrov, M.P. Kirpichnikov, K.V. Shaitan, Application of the Johnson–Kendall–Roberts model in AFM-based mechanical measurements on cells and gel, *Colloids Surf. B* 134 (2015) 131–139.
- [30] D. Tabor, Surface forces and surface interactions, *J. Colloid Interface Sci.* 58 (1977) 2–13.
- [31] S. B efahy, et al., Stretchable gold tracks on flat polydimethylsiloxane (PDMS) rubber substrate, *J. Adhes. Sci. Technol.* 84 (2008) 231–239.
- [32] K. Thorwarth, et al., HiPIMS titanium metallization of PEEK for improved osseointegration, *Eur. Cells Mat.* 30 (2015) 10.
- [33] Y.J. Yang, H.K. Tsou, Y.H. Chen, C.J. Chung, J.L. He, Enhancement of bioactivity on medical polymer surface using high power impulse magnetron sputtered titanium dioxide film, *Mater. Sci. Eng. C* 57 (2015) 58–66.
- [34] B. Osmani, H. Heyhle, T. T opper, T. Pfohl, B. M uller, Gold layers on elastomers near the critical stress regime, *Adv. Mater. Technol.* 2 (2017) 1700105.